Received: 24 November 2025 | Revised: 20 February 2026 | Accepted: 22 February 2026

DOI: 10.1002/alz.71351

Alzheimer's & Dementia®
THE JOURNAL OF THE ALZHEIMER'S ASSOCIATION

RESEARCH ARTICLE

Imaging the later-life white matter pathologies of repetitive head impacts: A novel pattern revealed through T2 FLAIR MRI

Jenna R. Groh[1,2] | Annalise E. Miner[1,2] | Mohamad J. Alshikho[3] | Chad Farris[2,4,5] | Anna Cui[1,2] | Erika Pettway[1,2] | Jacob Labonte[1,2] | Sydney Mosaheb[1,2] | Yorghos Tripodis[2,6] | Charles H. Adler[7] | Laura J. Balcer[8,9] | Charles Bernick[10] | Robert C. Cantu[2] | Michael J. Coleman[11] | David W. Dodick[7] | Nicholas J. Ashton[12,13,14] | Henrik Zetterberg[12,15,16,17,18,19] | Kaj Blennow[12,19] | Elaine R. Peskind[20,21] | Christopher Nowinski[2,22] | Monica Ly[1,2,23] | Caroline Altaras[1,2,23] | Steven Lenio[1,2,23] | Gil D. Rabinovici[24,25] | Breton Asken[26,27] | Howard Rosen[24,25] | Yann Cobigo[24,25] | Jan Krzysztof Blusztajn[28] | Andrew E. Budson[1,2,29] | Katherine Turk[2,29] | Wei Qiao Qiu[2,30,31] | Lee Goldstein[2,32,33] | Brett Martin[2,34] | Joseph N. Palmisano[2,34] | Diane Dixon[2,34] | Greta Schneider[2,34] | Eric G. Steinberg[2] | Yi Su[35] | Hillary Protas[35] | Ofer Pasternak[11] | Inga Koerte[11] | Sylvain Bouix[36] | Jeffrey L. Cummings[37] | Eric M. Reiman[35,38,39] | Martha E. Shenton[11,40] | Robert A. Stern[1,2,41,42] | Ann C. McKee[1,2,28,29,43] | Thor D. Stein[2,28,29,43] | Adam M. Brickman[3] | Jesse Mez[1,2,23,44] | Michael L. Alosco[1,2,23,41]

Correspondence
Jenna R. Groh, PhD, Boston University Chobanian & Avedisian School of Medicine, 72 E. Concord Street, Instructional Building, L-5, Boston, MA 02118, USA.
Email: jengroh@bu.edu

Funding information
NIA, Grant/Award Numbers: P30AG072978, R01AG083735; NINDS/NIA, Grant/Award Numbers: R01NS122854, R01NS139383; Department of Defense, Grant/Award Number: HT9425-24-1-1046

Abstract

INTRODUCTION: Repetitive head impacts (RHI) from contact sports may cause a unique pattern of white matter hyperintensities (WMH) on T2-weighted fluid-attenuated inversion recovery (FLAIR) magnetic resonance imaging (MRI), termed RHI-associated WMH (RHI-WMH). These lesions are punctate, circular, and located at the gray–white matter boundary, an area vulnerable to trauma-related damage.

METHODS: We investigated the association of RHI with these lesions in two aging cohorts: (1) former American football players versus asymptomatic unexposed men and (2) individuals with RHI from various contact sports versus non-RHI participants. RHI-WMH were assessed using visual ratings and a novel automated quantification pipeline.

RESULTS: Individuals with RHI had greater RHI-WMH by both detection methods in both cohorts. RHI-WMH were associated with plasma neurofilament light and p-tau231, and flortaucipir positron emission tomography (PET) uptake.

DISCUSSION: RHI-WMH may represent a new supportive biomarker for the detection of RHI-related neuropathologies later in life.

KEYWORDS
CTE, head injury, repetitive head impacts, sports, white matter injury

Highlights

- Repetitive head impacts (RHI) are associated with white matter and vascular pathology.
- T2-weighted fluid-attenuated inversion recovery (FLAIR) magnetic resonance imaging (MRI) of RHI-exposed participants revealed a unique pattern of white matter hyperintensities (WMH) quantified by visual ratings and an automated pipeline in two separate cohorts.
- These RHI-associated WMH correlated with plasma neurofilament light chain (NfL), hyperphosphorylated tau 231 (p-tau231), and tau positron emission tomography (PET).
- RHI-WMH offer a potentially valuable tool for clinical assessment and detection of RHI-related neurological conditions.

1 | BACKGROUND

Repetitive head impacts (RHI) from contact and collision sports can have long-term effects on brain health.[1,2] RHI do not always manifest in immediate clinical symptoms (i.e., concussion) but may result in brain injury and are associated with increased risk of neurodegenerative diseases later in life such as chronic traumatic encephalopathy (CTE).[3,4] CTE is a neuropathological diagnosis characterized by the abundance of neuronal hyperphosphorylated tau (p-tau) around small blood vessels at the depths of the sulci.[5–8] Those diagnosed with CTE at autopsy may have exhibited an array of clinical symptoms during life, including cognitive impairment and/or neurobehavioral dysregulation.[9,10] Cognitive symptoms are associated with CTE p-tau neuropathology but the neuropsychiatric symptoms weakly correlate with p-tau.[10,11] Other neuropathologies associated with RHI beyond p-tau may contribute to clinical symptoms, such as chronic damage to the white matter including axonal injury and myelin loss.[12]

Autopsy studies show RHI has substantial white matter and vascular consequences that can be detected during life with routine MRI sequences.[12–15,16] White matter damage can be visualized on T2-weighted fluid-attenuated inversion recovery (T2-FLAIR) magnetic resonance imaging (MRI) as white matter hyperintensities (WMH).[17] WMH are non-specific, associated with aging, and typically presumed to be of vascular origin, such as small vessel disease, that often co-occur with neurodegenerative diseases.[17] WMH have long been associated with accelerated cognitive decline, neuropsychiatric symptoms, and risk for Alzheimer's disease (AD) and related dementias.[18,19] WMH also co-localize with pathology in brain regions characteristically affected in AD and frontotemporal lobar degeneration,[20–22] suggesting that the pattern, distribution, and appearance of WMH may provide greater specificity to underlying disease processes rather than a general or global WMH burden estimate.

Aging former American football players exhibit greater WMH burden compared to men without RHI exposure, independent of age and vascular risk factors, which is associated with symptoms of cognitive and functional impairment.[23,24] Among former football players, WMH correlated with cerebrospinal fluid (CSF) p-tau181, lower fractional anisotropy on diffusion tensor imaging, and reduced cortical thickness.[25] We recently introduced the hypothesis that RHI might result in a unique pattern of WMH on FLAIR MRI.[26] Anecdotally, we observed RHI-exposed individuals exhibit punctate WMH that tend to be small and circular at the depths of the sulci that are distinguishable from large, confluent periventricular WMH typically seen in aging, AD, and vascular contributions to cognitive impairment. The lesion location at the depths of the sulci near the gray/white matter junction corresponds to areas susceptible to trauma including p-tau deposition in CTE. We termed this pattern of small, spherical, discrete WMH near the cortex at the depths of the sulci: RHI-associated WMH (RHI-WMH) (Figure 1).

To date, RHI-WMH has only been informed by case series and anecdotal observations. The objective of this study was to empirically examine whether exposure to RHI is associated with a novel pattern of WMH on T2-FLAIR MRI. We visually rated T2-FLAIR scans for RHI-WMH as well as developed and applied an automated features pipeline to detect RHI-WMH in two independent cohorts as most conventional methods for WMH segmentation out total WMH volume or total number of lesions. The first cohort included former elite American football players with RHI exposure and asymptomatic men without any history of RHI or traumatic brain injury (TBI) exposure from the DIAGNOSE CTE Research Project (DxCTE).[27] The second cohort included aging former contact and collision sport athletes as well as aging individuals without RHI exposure (non-RHI) from the Boston University (BU) Alzheimer's Disease Research Center (ADRC). We hypothesized that exposure to RHI would be associated with a greater number of RHI-WMH in both cohorts. In DxCTE, we tested the associations of RHI-WMH with plasma biomarkers, tau PET (18F-flortaucipir), and clinical outcomes.

RESEARCH IN CONTEXT

1. **Systematic review**: Neuroimaging and autopsy studies of contact sport athletes show that repetitive head impacts (RHI) are associated with white matter and vascular pathology. The present study is the first to characterize specific features of white matter hyperintensities (WMH) on T2-weighted fluid-attenuated inversion recovery (FLAIR) magnetic resonance imaging (MRI) in individuals with RHI exposure.
2. **Interpretation**: RHI exposure was associated with a distinct pattern of WMH, termed RHI-associated WMH (RHI-WMH). These lesions correlated with plasma neurofilment light chain (NfL), hyperphosphorylated tau 231 (p-tau231), and tau positron emission tomography (PET). These findings suggest that RHI-WMH reflect trauma-related pathology.
3. **Future directions**: Additional research is needed to (a) evaluate longitudinal change in RHI-WMH and its relationship to cognitive and functional decline; (b) integrate diffusion MRI and quantitative susceptibility mapping to further characterize microstructural and vascular features of RHI-WMH; (c) expand neuropathological-imaging correlation studies to determine the range of cellular substrates underlying these lesions.

2 | METHODS

2.1 | Study design and participants

The sample included two independent aging cohorts of research participants: (1) former professional and collegiate American football players ($n = 164$) and asymptomatic unexposed men without RHI or TBI history ($n = 55$) from the DxCTE Research Project, and (2) people with ($n = 38$) and without RHI exposure ($n = 38$) from the BU ADRC Clinical Core Cohort. Each dataset was analyzed separately. DxCTE recruited former elite American football players considered high risk for CTE, as well as a comparison group of participants who were asymptomatic and had no exposure to RHI or TBI.[28] The BU ADRC enrolls participants who span the continuum of exposure to RHI (in terms of type, frequency, and intensity) and a comparison group of people with minimum to no exposure to RHI. A brief overview of each study is provided below.

2.2 | Cohort 1: The DxCTE Research Project (DxCTE)

The DxCTE Research Project was supported by a National Institutes of Health U01 award that included four U.S. clinical sites. A detailed description of DxCTE is provided elsewhere.[28] The objectives of DxCTE were to characterize the clinical presentation and development of in vivo biomarkers of CTE. The DxCTE sample included 180 former football players (120 professional and 60 college players), and 60 asymptomatic unexposed men. All participants were between the ages of 45–74. The current sample size was reduced because of missing or incomplete T2-FLAIR sequences ($n = 13$), or for poor scan quality rendering the sequence unusable ($n = 4$). Four asymptomatic unexposed men were removed from the analysis after additional information at their follow-up visit, which was not disclosed during their screening visit, made them ineligible. The final sample included 164 former football players (111 professional and 53 college) as well as 55 asymptomatic unexposed men without RHI or TBI exposure. All participants in the study were required to have an informant and adequate capacity to consent to participate. All participant evaluation site institutions and associated sites received approval for study procedures by their governing instutional review board (IRB). All participants were provided written informed consent.

2.2.1 | MRI acquisition

MRI data were acquired with a Siemens 3T MAGNETOM Skyra (Erlangan, Germany; software version VE11) at all four sites. Quality control procedures have previously been described.[28] Structural MRI included T1-weighted rapid acquisition gradient echo structural sequences (repetition time [TR]/echo time [TE]/inverion time [TI] = 2530/3.36/1100 ms, voxel size = 1 × 1 × 1 mm) and T2-FLAIR (TR/TE/TI = 5000/388/1800 ms; voxel size = 1 × 1 × 1 mm).

2.2.2 | Tau and amyloid PET

[F18]-Flortaucipir tau PET (FTP) and Florbetapir amyloid PET data were available for the DxCTE cohort. Quality control, acquisition

procedures, and processing have been described elsewhere.[29–32] For FTP, three prespecified regions of voxel clusters defined in our previous study were generated and included: bilateral superior frontal region (2887 voxels), bilateral medial temporal region (1283 voxels), and left parietal region (252 voxels).[29,33] A positive florbetapir PET scan was defined by an average cortical standardized uptake value ratio (SUVR) of 1.10 or greater (Centiloid values > 24.3). Additional methods have been previously published.[34]

2.2.3 | Plasma biomarkers

Methods for collection, processing and analysis of plasma blood samples have been published.[35,36] Participants completed fasting blood draws (12 h) at their study visit. Samples were measured for beta-amyloid 42/40 ratio (Aβ42/Aβ40), phosphorylated tau 181 & 231 (p-tau181 & p-tau231), neurofilament light (NfL), and glial fibrillary acidic protein (GFAP). These were a priori selected.[37–39] The ratio of Aβ42/Aβ40, p-tau231, and p-tau181 were included based on their use for the detection and monitoring of AD/ADRD.[40,41] Additional information about assays can be found in Supplementary Materials.

2.2.4 | Clinical outcomes

Traumatic encephalopathy syndrome (TES) is the research diagnostic criteria for the clinical syndrome presumed to result from CTE.[42] TES diagnoses (yes/no) and TES provisional level of certainty for CTE (TES-CTE suggestive, TES-CTE possible, and TES-CTE probable) were assigned at multidisciplinary diagnostic consensus conferences, based on the 2021 NINDS TES Research Diagnostic Criteria.[42] Participants were administered the Montreal Cognitive Assessment (MoCA) to evaluate global cognitive function, the Functional Activities Questionnaire (FAQ) to assess instrumental activities of daily living, and the Cognitive Change Index (CCI) to measure self-reported cognitive change. These measures were selected in this analysis to test the association between global clinical outcomes and RHI-WMH.

2.3 | Cohort 2: BU ADRC Clinical Core Cohort (BU ADRC)

The BU ADRC longitudinally follows older adults with and without RHI to study the long-term effects of RHI and differentiate between CTE and AD and related dementias.[43] Participants span the cognitive spectrum and are recruited based on RHI exposure status. Participants were administered annual assessments. Additional standardized self-report measures include other neuropsychiatric, cognitive, and daily functioning measures, as well as comprehensive lifetime and head trauma characterization using the BU Repetitive Head Impact Exposure Assessment.[44–46] MRI is completed at baseline and 3-year follow-up. Biomarkers harmonized to DxCTE were not available in BU ADRC cohort, and therefore, the BU ADRC cohort analyses were limited to group comparisons of RHI-WMH. All procedures were approved by the BU Medical Campus Institutional Review Board and written informed consent was obtained for all participants or their legally authorized representatives.

Weekly multidisciplinary diagnostic consensus conferences involving neuropsychologists, neurologists, and neuroradiologists were conducted to review clinical histories, neuropsychological data, and biomarkers to reach consensus syndromal and etiological diagnoses for each participant. During consensus meetings, RHI exposure was evaluated using the BU Repetitive Head Impact Exposure Assessment and RHI group assignment was made following the 2021 TES research diagnostic criteria.[42,44,47,48] The RHI group includes individuals with "substantial" exposure, as defined by the TES criteria, primarily from contact and collisions sports such as boxing, American football, ice hockey, mixed martial arts, men's lacrosse, Greco-Roman wrestling, and rugby. The non-RHI group could include individuals with some history of RHI; however, their exposure level did not meet the "substantial" exposure threshold for inclusion in the RHI group.[49]

This study considered all participants from the BU ADRC with MRI completed as of November 7, 2023. When multiple scans were available, the baseline scan was used. From this pool of eligible participants, a matched dataset was created by pairing individuals 1:1 based on age (± 1 year) and sex. Initially, 88 participants were included in the matched sample. Six participants were excluded from the dataset because they were missing either a T1 or T2-FLAIR sequence and subsequently, we removed their matched counterpart ($n = 6$). Therefore, the final sample included 76 participants (38 RHI, 38 non-RHI).

2.3.1 | MRI acquisition

Scans were acquired on a Philips 3T Ingenia Elition (or Philips 3T Achieva prior to 2020) at Boston University's Center for Translational Neuroimaging. Structural MRI included sagittal 3D MPRAGE (TR/TE = 6.5/2.9 ms; flip angle = 9°; voxel size = 1 × 1 × 1 mm) and sagittal 3D T2-FLAIR (TR/TE/TI = 4800/271/1650 ms; voxel size = 1 × 1 × 1.2 mm).

2.4 | RHI-WMH visual counts

A novel visual rating system was developed to count RHI-WMH on T2-FLAIR in both cohorts. Visual counts were done to provide an initial review and characterization of the WMH pattern that was anecdotally visualized in consensus conferences (Figure 1). Automated pipelines used for the detection of WMH typically provide global metrics (e.g., total volume) but fail to capture the heterogeneous features of different types of WMH.[50,51] Established visual rating scales of WMH, including the Fazekas or Scheltens scales, do not capture specific features of WMH such as distance to the cortex, volume/size of individual lesions, or sphericity/confluence.[52,53] Because none of the existing visual scales capture the pattern of RHI-WMH (Figure 1), we developed a system to count the number of RHI-WMH, within 1.0 cm of the cortex

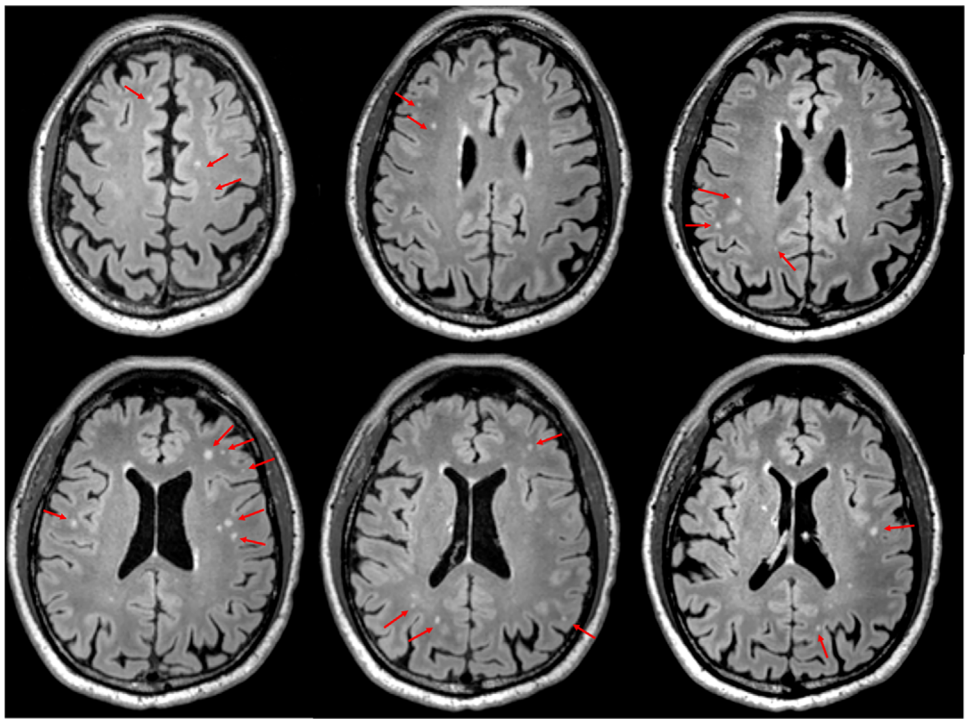

FIGURE 1 T2-FLAIR scan from a participant with substantial RHI exposure: Exemplar images of RHI-WMH. This figure, taken from Miner and Groh et al., displays the small, spherical punctate lesions close to the gray matter, distributed throughout the cortex, often in the absence of confluent periventricular lesions.[26] Lesions are also observed in relatively younger aged (e.g., 50s) individuals with minimal vascular risk factors. RHI, repetitive head impacts; T2-FLAIR, T2-weighted fluid-attenuated inversion recovery; WMH, white matter hyperintensities.

near the depths of the sulci. This method was developed by a board-certified neuroradiologist (C.W.F.), neuropsychologist with a CTE/RHI content specialization (M.L.A.), and advanced neuroscience PhD student (J.R.G.). Our complete visual rating manual can be found in Figure S1, but we briefly discuss our methods below.

To visualize the scans, we used the freely available viewing software Horosproject.org. 3D T2-FLAIR images were viewed in axial orientation and the number of RHI-WMH on each slice was counted. RHI-WMH were counted if they were small and circular in shape, distinguishable from large and confluent periventricular WMH, and within 1.0 cm of the cortex near depths of the sulci. We required the WMH to be at least as bright as the cortex to limit noise from varying resolution. Some WMH appeared on multiple slices; in these instances, we counted only the first appearance, flipping back and forth, slice-to-slice, and viewing the scan in all three planes, to determine if the position of the WMH remained the same. If the WMH was visualized on one axial slice, but not present on the next slice, and then reappeared in a similar location on the third slice, we counted that as two unique WMH. Once these features were established and defined, we counted the total number of WMH within 0.5 and 1.0 cm of the cortex informed by our hypothesis that WMH closer to the cortex are more specific to RHI. We used the Horos length tool to measure 0.5 and 1.0 cm from the cortex to count each individual WMH and marked them as they were counted to avoid duplicate counting. WMH within 1.0 cm is a total count within 1.0 cm from the cortex and includes all WMH within 0.5 cm of the cortex as well.

This novel visual rating system was developed using the BU ADRC dataset. One rater (J.R.G.) met with board-certified neuroradiologist (C.W.F.) to define the features, train on an initial set of 10 scans, and develop the visual counts manual. After initial training, an additional meeting occurred between J.R.G. and C.W.F. to further define features and revise the visual counts manual for clarification. Once initial training was completed, one rater (J.R.G.) rated all scans from the BU ADRC.

For the DxCTE dataset, two additional raters were trained on the method (A.E.M. and A.C.). To verify interrater reliability and consistency of measurement for this new method, all four raters (J.R.G., C.W.F., A.E.M., and A.C.) counted RHI-WMH on 15 randomly selected practice scans. We assessed the inter-rater reliability (IRR) using intraclass correlation coefficient (ICC) estimates with a two-way mixed-effects model (absolute agreement, mean rating) for both RHI-WMH within 0.5 and 1.0 cm of the cortex. The IRR for the initial 15 scans was "*good*" for the number of RHI-WMH within 0.5 cm of the cortex (ICC = 0.765, 95% confidence interval [CI]: 0.520–0.907), and "*good*" for the number of WMH within 1.0 cm (ICC = 0.840, 95% CI: 0.654–0.939) between the raters. In order to improve IRR, re-training with the neuroradiologist, CWF, was completed. An additional 10 randomly selected practice scans from the DxCTE cohort were counted by all four raters. The IRR for the secondary set of 10 scans improved and was "*good*" for the number of RHI-WMH within 0.5 cm of the cortex (ICC = 0.869, 95% CI: 0.698–0.961), and "*excellent*" for the number of WMH within 1.0 cm (ICC = 0.940, 95% CI: 0.834–0.980) between

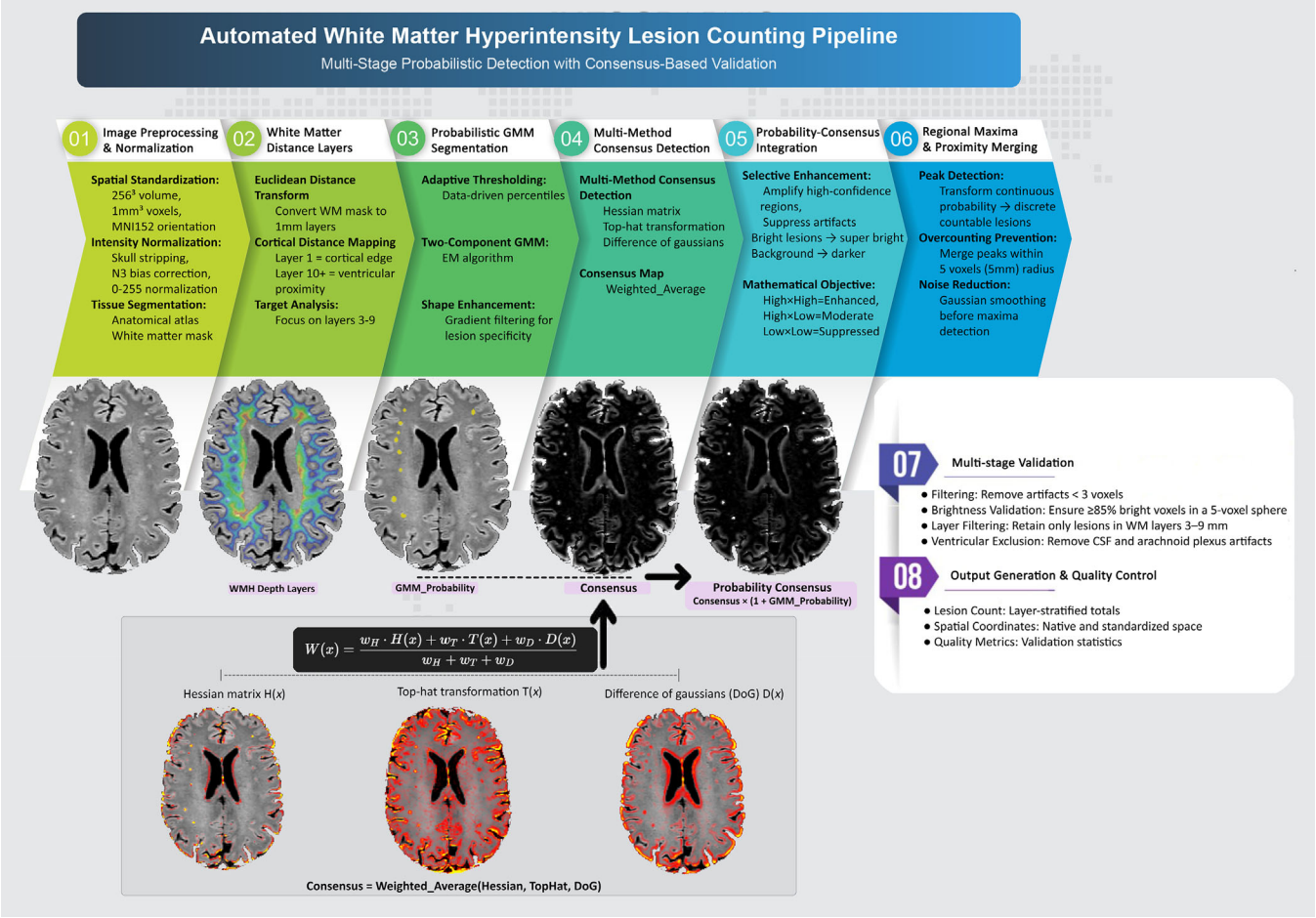

FIGURE 2 Automated white matter hyperintensity lesion counting pipeline methods schematic overview. This figure illustrates the preprocessing, lesion detection, and post-processing steps used to identify RHI-WMH on T2-FLAIR MRI. Preprocessing includes spatial standardization to MNI152 space, intensity normalization, and tissue segmentation using a white matter mask. Cortical distance mapping is performed using a Euclidean distance transform to stratify white matter into 1 mm layers, with lesion detection focused on layers 3–9 mm from the cortical surface. Lesions are identified through adaptive thresholding, a two-component GMM, and multi-method consensus detection using Hessian matrix, top-hat transformation, and difference-of-Gaussians filtering. A consensus probability map is created and refined via selective enhancement. Final lesion counts are extracted following peak detection, artifact suppression, and exclusion of lesions < 3 voxels or near ventricles. Output includes lesion counts, spatial coordinates, and quality control metrics. GMM, Gaussian mixture model; RHI, repetitive head impacts; T2-FLAIR, T2-weighted fluid-attenuated inversion recovery; WMH, white matter hyperintensities.

the raters. Once excellent agreement was established, all of the DxCTE scans for the second cohort were divided amongst three raters (J.R.G., A.E.M., A.C.) for counting.

2.5 | Automated pipeline methods

In addition to visual counts, we developed and implemented a novel automated WMH segmentation pipeline to provide standardized and highly sensitive WMH detection that reduced potential for user variability, and time demands inherent to visual ratings. Using the automated pipeline alongside visual counts combined objective quantification with expert interpretation, enhancing reproducibility and detection of subtle lesions. Our automated pipeline combined the output of three detection methods that each targeting distinct features of WMH. The steps are summarized in Figure 2.

This process begins with T2-FLAIR skull stripping, N3 bias-field correction, intensity normalization, and resampling to 1 mm^3. White matter is segmented and parcellated into 1 mm depth bins via Euclidean distance transformations from the cortical gray–white boundary toward the ventricles.[54] This structure enables lesion counts within specific white matter depths, reflecting the observed spatial distribution of WMH pathology in RHI.

The detection stage addresses three WMH characteristics. (1) Morphology: Hessian eigenvalue analysis distinguishes spherical punctate foci (three negative eigenvalues) from sheet-like confluent lesions (two negative eigenvalues) while suppressing tubular vessels and random noise.[55,56] (2) Contrast: subtle punctate lesions (<3–5 mm) are enhanced using morphological white top-hat filtering with a structuring element tuned to ≈3–4 mm after resampling, which amplifies small hyperintense foci while suppressing gradual intensity variations. (3) Scale: because WMH span punctate (<3–5 mm), focal (3–12 mm),

and early-confluent/confluent (>12 mm) extents without a universal upper limit, Difference-of-Gaussians filtering with sigma≈1 mm and ≈3 mm isolates features in the punctate/small-focal range while attenuating noise and large-scale gradients.[57,58] All detector maps are percentile-clipped (1st–99th, nonzero voxels) and normalized to [0,1]. Detector outputs are combined by confidence-weighted averaging, using each method's own normalized score as its weight (with a small constant added to avoid zero contribution). The consensus map is then probability-refined by integrating voxel-wise lesion segmentation posteriors from a Gaussian Mixture Model (GMM): multiplying by (1 + posterior) and renormalizing to [0,1] provides a probability-weighted contrast enhancement, up-weighting high-probability voxels and suppressing residual noise.

Individual lesions are delineated via regional-maxima detection.[59] To avoid over-counting, peaks located within 5 mm of each other are merged so that multiple nearby foci are counted as a single lesion. Size, brightness, ventricular-adjacent, and depth constraints remove spurious detections, with counts restricted to white-matter bins of interest. The pipeline outputs lesion counts and distributions stratified by depth bins, reducing detector-specific bias while enabling depth-resolved WMH quantification.

2.6 | Statistical analyses

All analyses were conducted using R (v4.1.2). The total number of RHI-WMH (visual and automated counts) was square-root transformed due to the non-normal distribution of residuals. Plasma and tau PET analyses were adjusted for multiple comparisons using the Benjamini–Hochberg false discovery rate (FDR) method with significance set at an adjusted *p*-value of 0.05. *p*-values were corrected by the number of items per biomarker domain for plasma biomarkers.

2.6.1 | Cohort 1: DxCTE

Covariates

All DxCTE analyses included a priori selected covariates: age at MRI, race, and vascular risk factors (presence/absence of sleep apnea, and the revised Framingham Stroke Risk Profile (rFSRP).[60] Race was included as dichotomized variable (White vs. non-White) due to a limited number of participants identifying as races other than White or Black/African American. As noted previously, MRI data for DxCTE were acquired at four different sites using the same scanner type across site locations, with identical acquisition parameters applied at each scanner. Scanner site was included as a covariate in the automated pipeline analyses to account for any potential variability related to scanner; however, it was not included in the visual count analyses because the counts were performed by the same trained raters using standardized criteria.

RHI-WMH visual counts

Analysis of covariance (ANCOVA) tested group differences in RHI-WMH (0.5 and 1.0 cm) between former football players and asymptomatic unexposed men. Additional ANCOVAs examined differences between former professional and former college football players. Among the former football players, linear regression models tested the association between RHI-WMH and metrics of RHI, including age of first exposure[61] and years of football play.[4] Models examining age of first exposure included total years of play as a covariate.

Biomarkers and clinical correlates

Among former football players, linear regressions evaluated relationships between RHI-WMH and tau PET composite SUVR scores, plasma biomarkers (p-tau181, p-tau231, NfL, GFAP, Aβ42/40), and clinical measures (MoCA, CCI, and FAQ). MoCA models included education as a covariate. TES group differences (yes/no, level of certainty) in RHI-WMH count were assessed by ANCOVA with post hoc Tukey comparisons and estimated marginal means (EMM).

Sensitivity analyses

We repeated all group level comparisons with the Headache Impact Test (HIT-6) total score added as an additional covariate, as well as after excluding amyloid PET positive individuals (defined by 1.10 or greater SUVR). To evaluate the incremental value of the RHI-WMH metric relative to conventional white matter hyperintensity measures, we conducted sensitivity analyses incorporating total lesion volume (TLV) as an additional covariate in the primary models.[23,50] These analyses tested whether the RHI-WMH pattern explained variance in exposure group membership beyond that accounted for by global WMH burden.

2.6.2 | Cohort 2: BU ADRC

Covariates

All analyses in the BU ADRC cohort included a priori selected covariates: age at MRI, race, and vascular risk factors (presence/absence of sleep apnea, and hypertension). The rFSRP was not available for BU ADRC cohort. Race was included as dichotomized variable (White vs. non-White) due to a limited number of participants identifying as races other than White or Black/African American.

RHI-WMH visual counts

We compared the total number of visually rated RHI-WMH between RHI and non-RHI groups using ANCOVA. Separate models examined RHI-WMH within 0.5 and 1.0 cm of the cortex. We tested the association between RHI-WMH count and total years of football play using linear regression. Among the former football players, linear regression models tested the association between RHI-WMH and age of first exposure, including total years of play as a covariate.

2.7 | Automated detection of RHI-WMH

For both the DxCTE and the BU ADRC cohort, the same ANCOVA models compared automated RHI-WMH counts between exposure groups.

We conducted a Pearson correlation between the visual RHI-WMH count (0.5 and 1.0 cm) and the pipeline-derived RHI-WMH count.

3 | RESULTS

3.1 | Cohort 1: DxCTE sample characteristics

Table 1 summarizes sample characteristics and demographic data. The average age of the entire sample was 58.0 (*SD* = 8.41). Former football players and asymptomatic unexposed men did not differ in age, race, or education; however, racial composition differed across the three exposure groups (former professionals, college players, and asymptomatic unexposed men). Vascular risk factors among the former football players and asymptomatic unexposed men included the following: football players had higher rates of sleep apnea ($p = 0.010$), but not atrial fibrillation ($p = 0.12$) or diabetes ($p = 0.54$). Asymptomatic unexposed men had higher stroke risk (rFSRP; $p < 0.001$). Among former players, the average MoCA was 24.7 (*SD* = 3.4), and FAQ was 3.4 (*SD* = 5.3). Of the former players, 36% (*n* = 58) were classified as TES-no, 20% (*n* = 32) TES-CTE Suggestive, 13% (*n* = 21) TES-CTE Possible, and 32% (*n* = 52) TES-CTE Probable.

3.1.1 | Raw visual counts of RHI-WMH

Before square-root transformation of visually counted RHI-WMH within 0.5 cm of the cortex, former football players had an average of 24.6 (*SD* = 44.0, range: 0–265) RHI-WMH, while asymptomatic unexposed men had an average of 12.0 (*SD* = 18.33; range: 0–89) RHI-WMH. Within 1.0 cm of the cortex, former football players had an average of 33.0 RHI-WMH (*SD* = 55.8, range: 0–294), whereas asymptomatic unexposed men had an average of 16.8 RHI-WMH (*SD* = 25.6, range: 0–128).

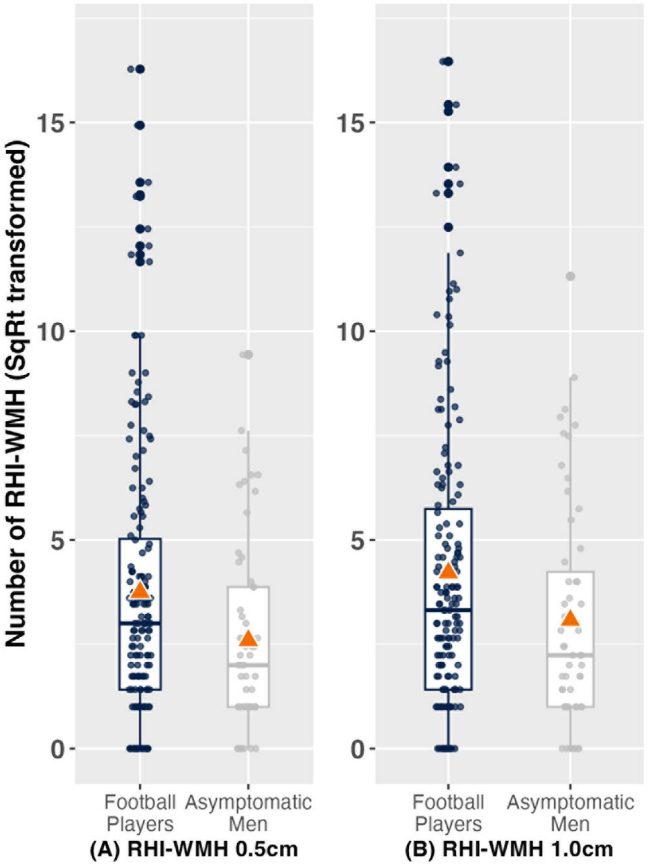

FIGURE 3 Visually counted RHI-WMH within 0.5 and 1.0 cm of the gray matter in the DxCTE Cohort. (A) The total number of RHI-WMH within 0.5 cm was significantly greater in football players compared to asymptomatic unexposed men ($p = 0.0003$). (B) The total number of RHI-WMH within 1.0 cm of the cortex was also greater in the former football players compared to the asymptomatic unexposed men ($p = 0.0004$). The box represents the interquartile range (IQR; 25th–75th percentile), the horizontal line inside the box indicates the median, and the whiskers extend to 1.5 × IQR. The orange triangle denotes the mean. IQR, interquartile range; RHI, repetitive head impacts; WMH, white matter hyperintensities.

3.1.2 | Group differences on visual counts of RHI-WMH

Former football players had significantly more RHI-WMH within 0.5 cm (EMM difference = 1.84, $p = 0.0003$) and 1.0 cm of the cortex (EMM difference = 1.99, $p = 0.0004$) compared to asymptomatic unexposed men (Table 2; Figure 3). Total years of play was not associated with RHI-WMH within 0.5 cm (standardized $\beta = -0.04$, $p = 0.628$, 95% CI [−0.15, 0.09]) or 1.0 cm (standardized $\beta = -0.03$, $p = 0.720$, 95% CI [−0.16, 0.11]) among former football players. Age of first exposure was not associated with RHI-WMH within 0.5 cm (standardized $\beta = -0.07$, $p = 0.370$, CI [−0.28, 0.11]) or 1.0 cm (standardized $\beta = -0.07$, $p = 0.396$, 95% CI [−0.31, 0.12]).

When examined by level of exposure, former professional players had more visually rated RHI-WMH compared to asymptomatic unexposed men within 0.5 and 1.0 cm of the cortex (EMM difference = 1.87, $p = 0.001$ & EMM difference = 2.05, $p = 0.002$, respectively). Former college players had more RHI-WMH compared to the asymptomatic unexposed men within 0.5 and 1.0 cm of the cortex (EMM difference = 1.77, $p = 0.018$ and EMM difference = 1.85, $p = 0.030$, respectively). There was no difference in number of RHI-WMH between the professional and college players at 0.5 or 1.0 cm of the cortex (EMM difference = 0.10, $p = 0.98$ and EMM difference = 0.20, $p = 0.95$, respectively) (Figure S2 and Table S1).

3.1.3 | Sensitivity analyses

All group differences in RHI-WMH remained statistically significant when HIT-6 was included in the models and after excluding amyloid PET positive individuals (*n* = 17). When total lesion volume was added to the models, former football players had significantly more RHI-WMH within 0.5 cm (EMM difference = 2.56, $p = 0.035$) and

TABLE 1 Sample characteristics of DxCTE cohort.

Parameter	Former football players $N = 164$[a]	Asymptomatic unexposed men $N = 55$[a]	p-value[b]
Demographics			
Age (years)	57.38 (8.34)	59.67 (8.44)	0.077
Education (years)	16.75 (1.46)	17.47 (3.50)	0.68
Race: (% non-White)	62 (38%)	21 (38%)	0.96
Athletic characteristics			
Total years of play	15.8 (4.3)	NA (NA)	–
Medical/vascular profile			
Sleep apnea	57 (35%)	9 (17%)	0.010
Diabetes	10 (6.2%)	5 (9.1%)	0.54
Revised Framingham Stroke Risk Profile	0.03 (0.03)	0.05 (0.04)	<0.001
Smoked > 100 cigarettes in lifetime	22 (13%)	15 (27%)	0.018
Atrial fibrillation	9 (5.6%)	0 (0%)	0.12
Systolic blood pressure	126.04 (12.24)	134.44 (13.75)	<0.001
High cholesterol	60 (37%)	26 (47%)	0.18
High blood pressure or hypertension	71 (44%)	25 (46%)	0.73
Myocardial infarction	3 (1.9%)	1 (1.8%)	>0.99
Cardiac arrest	0 (0%)	0 (0%)	>0.99
Coronary artery disease	14 (8.6%)	2 (3.6%)	0.37
Congestive heart failure	0 (0%)	0 (0%)	>0.99
Angina	1 (0.6%)	0 (0%)	>0.99
Peripheral vascular disease	3 (1.8%)	1 (1.8%)	>0.99
Angioplasty	5 (3.1%)	2 (3.6%)	>0.99
Cardiac bypass surgery	1 (0.6%)	0 (0%)	>0.99
Valvular heart disease	2 (1.2%)	1 (1.8%)	>0.99
Clinical characteristics			
HIT-6 total score	46.65 (10.29)	40.09 (5.33)	<0.001
FAQ total score	3.4 (5.3)	0.2 (0.5)	<0.001
CCI total score	32 (13)	14 (2)	<0.001
MoCA (raw total score)	24.7 (3.4)	26.7 (1.9)	<0.001
Florbetapir PET positive[c]	14 (8.6%)	3 (5.7%)	0.77
Diagnoses			
TES—Dementia			<0.001
Independent—No Dementia	98 (60%)	54 (98%)	
Subtle/mild functional limitation	53 (32%)	1 (1.8%)	
Mild dementia	13 (7.9%)	0 (0%)	
TES Level of CTE certainty			<0.001
No TES	58 (36%)	55 (100%)	
Suggestive of CTE	32 (20%)	0 (0%)	
Possible CTE	21 (13%)	0 (0%)	
Probable CTE	52 (32%)	0 (0%)	

Abbreviations: CCI, Cognitive Change Index; CTE, chronic traumatic encephalopathy; DxCTE, DIAGNOSE CTE Research Project; FAQ, Functional Activities Questionnaire; HIT-6, Headache Impact Test-6; MoCA, Montreal Cognitive Assessment; RHI-WMH, repetitive head impact associated white matter hyperintensities; SUVR, standardized uptake value ratio; TES, traumatic encephalopathy syndrome.

[a]Mean (SD); n (%).

[b]Wilcoxon rank sum test; Pearson's chi-squared test; Fisher's exact test.

[c]Positivity defined by SUVR of 1.10 or greater.

TABLE 2 Group differences in visual and automated counts of RHI-WMH between former football players and asymptomatic unexposed (UE) men from the DIAGNOSE CTE Research Project (DxCTE) cohort.

				95 % CI		
Parameter	**Exposure**	**EMM**	**SE**	**Lower**	**Upper**	***p*-value**
Visual counts (0.5 cm)	Football	4.06	0.25	3.56	4.56	0.0003
	Asymptomatic UE Men	2.22	0.45	1.34	3.11	
Visual counts (1.0 cm)	Football	4.67	0.29	4.12	5.23	0.0004
	Asymptomatic UE Men	2.68	0.50	1.69	3.67	
Automated counts	Football	2.87	0.16	2.55	3.18	0.006
	Asymptomatic UE Men	1.99	0.28	1.44	2.55	

Note: Estimated marginal means (EMM) and standard error (SE) of repetitive head impact associated white matter hyperintensities (RHI-WMH), assessed via visual counts at 0.5 and 1.0 cm of the cortex and automated counts, are presented for former football players and asymptomatic unexposed men. Group differences were evaluated with 95% confidence intervals (CI) and corresponding *p*-values. Significantly higher RHI-WMH burden was observed in former football players via both methods of RHI-WMH counts.

1.0 cm of the cortex (EMM difference = 2.53, $p = 0.028$) compared to asymptomatic unexposed men. When examining differences by level of exposure (professional vs. college vs. unexposed), effect size estimates remained similar in magnitude; however, the overall model no longer reached statistical significance, likely reflecting limited power given the small subgroup sample size. Pairwise contrasts demonstrated numerically higher RHI-WMH burden among exposed groups relative to unexposed asymptomatic men (Professional vs. Unexposed: EMM difference = 2.40, $p = 0.094$; College vs. Unexposed: EMM difference = 3.53, $p = 0.056$), whereas differences between professional and college players were small and non-significant (EMM difference = −1.13, $p = 0.431$). The RHI-WMH signal remains consistent after accounting for total lesion volume.

3.1.4 | Biomarker associations with visual counts RHI-WMH

Among former football players, higher plasma p-tau231 (standardized $\beta = 0.17$, SE = 0.47, $p_{adj} = 0.041$, 95% CI [0.17, 2.01]) and NfL (standardized $\beta = 0.18$, SE = 0.61, $p_{adj} = 0.028$, 95% CI [0.14–2.54]) concentrations were associated with more RHI-WMH within 0.5 cm (Figure 4) but p-tau181 (standardized $\beta = 0.08$, SE = 0.48, $p_{adj} = 0.295$, 95% CI [−0.44 to 1.45]), GFAP (standardized $\beta = -0.03$, SE = 0.82, $p_{adj} = 0.784$, 95% CI [−1.84 to 1.39]), and the ratio Aβ42/40 (standardized $\beta = -0.03$, SE = 19.21, $p_{adj} = 0.697$, 95% CI [−45.49 to 30.49]) were not.

Results were similar for associations within 1.0 cm: higher NfL (standardized $\beta = 0.18$, SE = 0.68, $p_{adj} = 0.034$, 95% CI [0.11, 2.78]) was associated with more RHI-WMH, but p-tau231 (standardized $\beta = 0.16$, SE = 0.52, $p_{adj} = 0.067$, 95% CI [0.10, 2.14]), p-tau181(standardized $\beta = 0.07$, SE = 0.53, $p_{adj} = 0.319$, 95% CI [−0.52 to 1.59]), GFAP (standardized $\beta = -0.03$, SE = 0.91, $p_{adj} = 0.771$, 95% CI [−2.07 to 1.53]), and the ratio Aβ42/40 (standardized $\beta = -0.03$, SE = 21.39, $p_{adj} = 0.692$, 95% CI [−50.78 to 33.79]) were not.

RHI-WMH within 0.5 cm was associated with composite tau PET SUVRs in the frontal (standardized $\beta = 0.18$, SE = 2.27, $p_{adj} = 0.046$, 95% CI [0.47–9.44]) and left-parietal (standardized $\beta = 0.17$, SE = 2.29, $p_{adj} = 0.046$, 95% CI [0.47–9.53]) cortex (Figure 4) but not the mesial-temporal lobe (standardized $\beta = 0.10$, SE = 1.87, $p_{adj} = 0.285$, 95% CI [−1.69 to 5.70]). RHI-WMH within 1.0 cm were not associated with tau PET SUVRs in the frontal (standardized $\beta = 0.17$, SE = 2.52, $p_{adj} = 0.060$), 95% CI [0.25–10.22], left-parietal (standardized $\beta = 0.17$, SE = 2.54, $p_{adj} = 0.060$, 95% CI [0.32–10.39]), or the mesial-temporal lobe (standardized $\beta = 0.09$, SE = 2.08, $p_{adj} = 0.323$, 95% CI [−2.04 to 6.17]).

3.1.5 | Clinical associations

Among former football players, a higher FAQ score (worse functioning) was associated with more RHI-WMH within 0.5 cm (standardized $\beta = 0.21$, SE = 0.05, $p = 0.008$, 95% CI [0.04–0.23]) and 1.0 cm (standardized $\beta = 0.21$, SE = 0.06, $p = 0.0074$, 95% CI [0.04–0.26]). MoCA total scores, CCI total scores and TES diagnoses were not associated with RHI-WMH.

3.2 | Cohort 2: BU ADRC

Sample characteristics and demographics are summarized in Table S2. Demographic and clinical characteristics were similar between groups. Clinical characteristics and vascular risk factors, including sleep apnea presence ($p = 0.21$), and hypertension ($p = 0.15$) did not differ between groups. The groups did not differ in terms of cognitive diagnoses; there were 21 participants total with mild cognitive impairment (RHI: 9, non-RHI: 12), and 10 participants with dementia (RHI: 5, non-RHI: 5). Among the RHI group, sources of RHI could be cumulative from participation in multiple sports which included the following: American football ($n = 29$), ice hockey ($n = 11$), soccer ($n = 17$), wrestling ($n = 4$), lacrosse ($n = 6$), mixed martial arts ($n = 1$), and rugby ($n = 2$).

3.2.1 | Raw visual counts of RHI-WMH

Before square-root transformation, RHI participants had an average of 21.61 visually counted RHI-WMH (*SD* = 22.89, range: 0–82) within 0.5 cm of the cortex and 31.63 RHI-WMH (*SD* = 31.56,

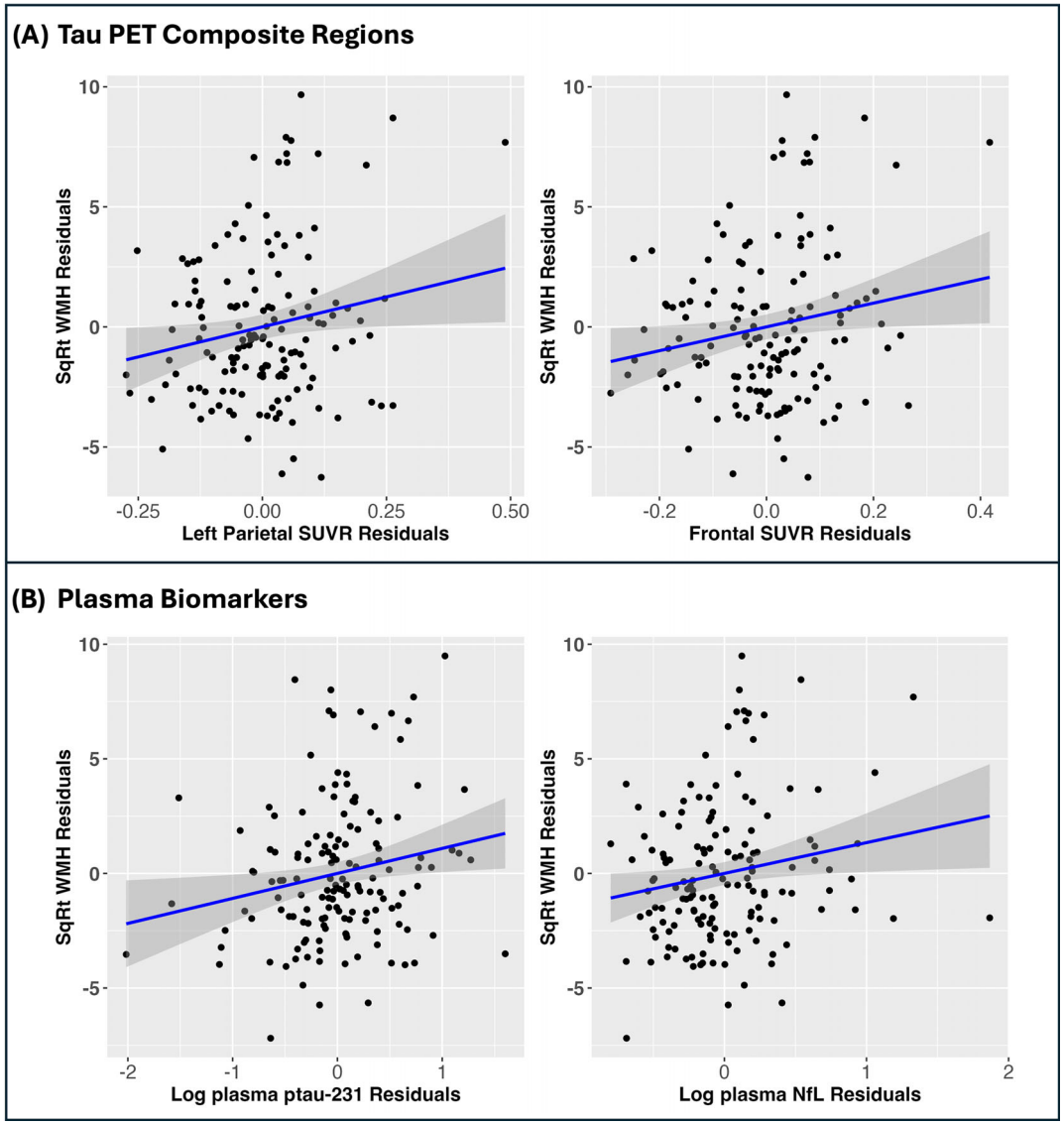

FIGURE 4 Adjusted associations between the number of RHI-WMH (visual) within 0.5 cm of the cortex and log-transformed plasma biomarkers/tau PET composite regions in the former American football players. Partial regression plots were adjusted for covariates: age, race, rFSRP, and sleep apnea. Significant associations include FTP composite SUVR regions left parietal (Panel A; standardized $\beta = 0.17$, $p_{adj} = 0.046$) and frontal SUVR (Panel A; standardized $\beta = 0.18$, $p_{adj} = 0.046$) and plasma p-tau231 (Panel B; standardized $\beta = 0.17$, $p_{adj} = 0.041$) and NfL (Panel B; standardized $\beta = 0.18$, $p_{adj} = 0.028$). FTP, [F18]-flortaucipir tau PET; NfL, neurofilament light chain; PET, positron emission tomography; rFSRP, revised Framingham Stroke Risk Profile score; RHI, repetitive head impacts; SUVR, standardized uptake value ratio; WMH, white matter hyperintensities.

range: 0–119) within 1.0 cm of the cortex. Non-RHI participants had an average of 9.11 visually counted RHI-WMH (*SD* = 13.64, range: 0–57) within 0.5 cm of the cortex, and 14.61 RHI-WMH (*SD* = 20.87, range: 0–78) within 1.0 cm of the cortex.

3.2.2 | Group differences on visual counts of RHI-WMH

RHI participants had more RHI-WMH compared to the non-RHI participants within 0.5 cm (EMM difference = 1.72, $p = 0.002$) and 1.0 cm (EMM difference = 2.01, $p = 0.002$) (Table S3, Figure S3). Total number of RHI-WMH at 0.5 and 1.0 cm from the cortex was associated with total years of football play (standardized $\beta = 0.34$, SE = 0.05, $p = 0.007$, 95% CI [0.04- 0.22] and standardized $\beta = 0.33$, SE = 0.05, $p = 0.010$, CI [0.04–0.25], respectively) (Figure 5). Total number of RHI-WMH at 0.5 and 1.0 cm from the cortex was not associated with age of first exposure to football (standardized $\beta = -0.02$, SE = 0.24, $p = 0.943$, 95% CI [0.53–0.50] and standardized $\beta = 0.06$, SE = 0.28, $p = 0.786$, 95% CI [−0.51 to 0.67], respectively.

Automated Detection of RHI-WMH: DxCTE and BU ADRC

There was strong correlation between the automated counts of RHI-WMH and the visual counts of RHI-WMH for both the DxCTE (0.5 cm: $r = 0.90$, 95% CI [0.87–0.92], $p < 0.0001$; 1.0 cm: $r = 0.91$, 95%

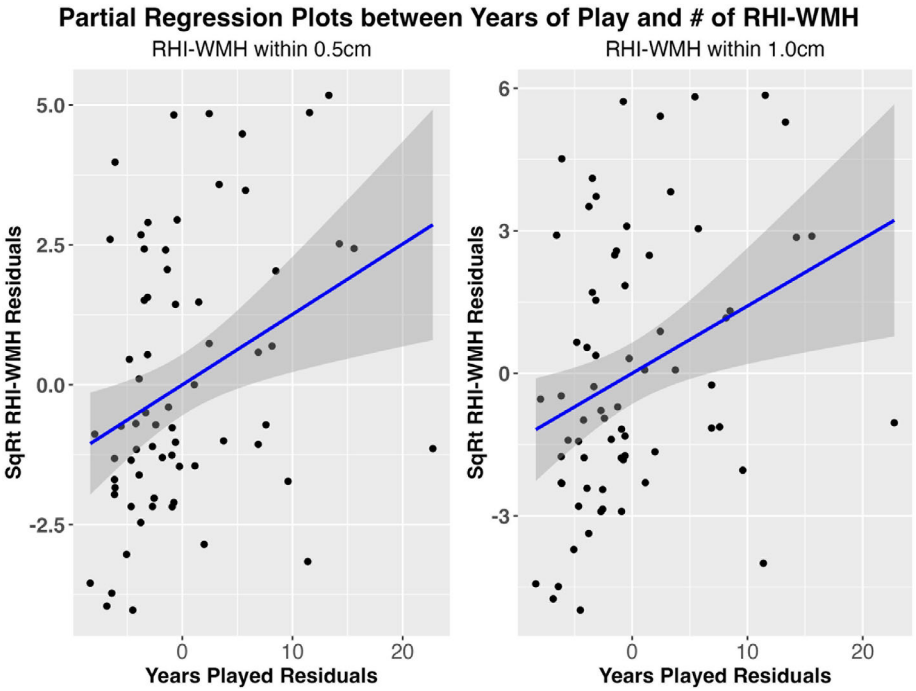

FIGURE 5 Adjusted associations between the number of RHI-WMH (square-root transformed) within 0.5 and 1.0 cm of the cortex and total years of football play in the BU ADRC Cohort. Partial regression plots were adjusted for covariates: age at MRI, race, hypertension, and sleep apnea. Years of play were significantly associated with the number of RHI-WMH within 0.5 cm (standardized $\beta = 0.34$, SE = 0.05, $p = 0.007$, 95% CI = 0.04–0.22) and within 1.0 cm (standardized $\beta = 0.33$, SE = 0.05, $p = 0.010$, 95% CI = 0.04–0.25) of the cortex. BU ADRC, Boston University Alzheimer's Disease Research Center; CI, confidence interval; MRI, magnetic resonance imaging; RHI, repetitive head impacts; WMH, white matter hyperintensities.

CI [0.89–0.93], $p < 0.0001$) and the BU ADRC cohort (0.5 cm: $r = 0.80$, 95% CI [0.70–0.87], $p < 0.0001$; 1.0 cm: $r = 0.84$, 95% CI [0.76–0.90], $p < 0.0001$) (Figure S4).

3.3 | Automated pipeline results

3.3.1 | Cohort 1: DxCTE raw automated counts of RHI-WMH

Before square-root transformation of automated counts RHI-WMH, former football players had an average of 11.6 RHI-WMH ($SD = 20.1$, range: 0–103) while asymptomatic unexposed men had an average of 7.7 RHI-WMH ($SD = 11.5$, range: 0–71). When broken down by exposure group, former professional football players had an average of 14.4 ($SD = 23.4$, range: 1–103) RHI-WMH and former college football player had an average of 5.8 ($SD = 8.0$, range: 0–37) RHI-WMH.

3.3.2 | Cohort 1: DxCTE group differences on automated counts of RHI-WMH

Former football players had a greater number of RHI-WMH compared to asymptomatic unexposed men (EMM difference = 0.87, $p = 0.006$) (Table 2). All group differences on RHI-WMH remained statistically significant when HIT-6 was included in the model and after excluding amyloid PET positive individuals. Number of RHI-WMH was significantly greater in former professional football players compared to asymptomatic unexposed men (EMM difference = 0.99, $p = 0.008$) but there was no difference between former college players and asymptomatic unexposed men (EMM difference = 0.59, $p = 0.30$), or between former professional and college players (EMM difference = 0.39, $p = 0.51$) (Table S1).

3.3.3 | Cohort 2: BU ADRC raw automated counts of RHI-WMH

Before square-root transformation of automated counts, RHI participants had an average of 20.16 RHI-WMH ($SD = 17.50$, range: 2–76), while non-RHI participants had an average of 12.71 RHI-WMH ($SD = 14.47$, range: 0–62).

3.3.4 | Cohort 2: BU ADRC group differences on automated counts of RHI-WMH

RHI-WMH detected by the pipeline was greater in RHI participants compared to non-RHI participants (EMM difference = 1.07, $p = 0.014$) (Table S3).

4 | DISCUSSION

Prior research has described greater WMH in former American football players, but here we assessed specific WMH characteristics beyond total volume.[23] We examined RHI-WMH in two independent aging cohorts, using both visual counts and a new automated pipeline. In the DxCTE cohort, former football players had more visual and automated counts of RHI-WMH than asymptomatic unexposed men, controlling for age, race, and cardiovascular risk factors. This finding was replicated in the BU ADRC Clinical Core Cohort; RHI exposed participants had more visual and automated counts of RHI-WMH than non-RHI individuals, controlling for age, race, and cardiovascular risk factors, with greater years of play associated with more RHI-WMH. In addition to group differences, among former players in the DxCTE cohort, the number of RHI-WMH correlated with plasma biomarkers reflecting p-tau pathophysiology (p-tau231) and axonal degeneration (NfL) as well as with 18F-FTP PET uptake across large, composite regions of interest (frontal and left parietal).

The greater number of RHI-WMH in former football players compared to asymptomatic unexposed men from the DxCTE cohort provides evidence of this pattern in elite athletes with substantial exposure. The BU ADRC provided an independent cohort of individuals with varying levels and types of RHI exposure beyond American football, in addition to a non-RHI comparison group who spanned the continuum of cognitive impairment ($n = 17$ with mild cognitive impairment [MCI]/dementia). The use of these cohorts is a notable strength of the study. Metrics of football exposure, total years of play and age of first exposure, were not significantly associated with RHI-WMH in the DxCTE cohort. The lack of association with years of play in the DxCTE may relate to a ceiling effect in this sample. The DxCTE cohort required > 12 years of play for the former professionals or a minimum of 6 years of play for the former college players for inclusion into the study. Within the BU ADRC cohort, we observed a significant association between years of play and RHI-WMH because this cohort had the entire spectrum of exposure (range: 0–25 cumulative years of play). The BU ADRC cohort also exhibited a wider range of types of exposure, providing support that RHI from sources beyond American football can contribute to white matter damage visible on T2-FLAIR MRI.

The presence of RHI-WMH at the gray-white matter interface is notable, as this anatomical stress point is vulnerable to trauma-related pathology. Neuropathological studies found axonal injury and white matter disruption at sulcal depths near hyperphosphorylated tau-positive regions in RHI-exposed brains, consistent with our DxCTE cohort where RHI-WMH correlated with plasma NfL, a marker of axonal injury.[13] Other studies showed that RHI exposure increases chronic microglial activation and neuroinflammation, which may partially mediate the pathways of developing hyperphosphorylated tau pathology.[62,63] The association between RHI-WMH and p-tau231 might also be of significance. Phosphorylation of amino acid 231 of tau has been specifically linked to tau pathology in TBI, especially the cis p-tau231 form.[64] While our assay does not differentiate cis and trans p-tau231, it is interesting to note that p-tau231 correlated more strongly with RHI-WMH than p-tau181. RHI-WMH likely reflect multiple neuropathologies related to RHI, including vascular injury, axonal damage, demyelination, and/or neuroinflammation, that may be up or downstream of tau-related neurodegeneration, warranting further imaging-pathological research. Future work will include a study of in vivo and ex vivo MRI–histopathology co-localization in a *post mortem* cohort, enabling more robust, lesion-level and quantitative analyses of the neuropathologic substrates underlying RHI-WMH.

RHI-WMH could be of potential aid to clinicians and increase suspicion for underlying neuropathologies related to RHI later in life. T2-FLAIR is a widely used imaging sequence in both research and clinical settings. We hypothesize that RHI-WMH closer to the gray/white matter junction are specific to RHI-related pathology. If an individual presents with cognitive or neurobehavioral dysfunction and has substantial RHI exposure, identifying this pattern could help provide support (albeit non-specific) that RHI exposure has contributed at least in part to clinical symptoms. This could be particularly useful because the clinical and biomarker presentation of CTE, for example, can mirror AD. While RHI-WMH is not going to be a biomarker for CTE, it could provide supportive data for RHI-related underlying processes. It is also important to note that RHI-WMH is distinct from patterns observed in AD/ADRDs as has been reviewed in detail elsewhere.[26]

RHI-WMH were present to a much lesser extent in the control groups. While we hypothesize that lesion location, that is, near the depths of the sulci within 1.0 cm of the cortex, is an important feature of RHI-WMH, the specificity of shape, exact size, and signal intensity, is not yet fully defined. We suspect that as we continue to study these lesions, we will further define these features to be more specific to RHI. As an example, our data suggest that proximity to the gray–white matter boundary will improve specificity. Additionally, many of the control participants had RHI-WMH in the context of moderate, confluent WMH (perhaps related to aging or disease). In the RHI groups, we often observe RHI-WMH in the absence of confluent WMH. Accounting for non-RHI-WMH lesions on T2-FLAIR in comparisons group will be important in future studies when examining and interpreting specificity to RHI. Furthermore, future studies leveraging larger, independent imaging cohorts (i.e., National Alzheimer's Disease Coordinating Center, NACC) with detailed characterization of RHI exposure will be critical for further establishing the specificity of RHI-WMH relative to vascular and neurodegenerative white matter pathology. Importantly, the newly implemented Uniform Data Set (UDS) Version 4.0 now includes structured queries assessing contact sports participation and RHI history, which will facilitate more rigorous exposure stratification and external validation of the RHI-WMH in future studies.

The ability to establish causal links and etiology of RHI-WMH is limited by the cross-sectional design of the study. Longitudinal studies assessing temporality of onset relative to RHI exposure and RHI-WMH change over time are needed to better understand if or how they evolve, which in turn may inform their etiology (e.g., static effects of prior RHI vs. a downstream progressive process). The DxCTE cohort included only men, and the BU ADRC cohort included only 16% women, limiting the generalizability of our findings based on sex. Additionally,

our study primarily included American football players. The BU ADRC included participants with exposures beyond American football; however, 34% of the cohort had exposure from football, which may restrict the broader applicability of these results. Further research is necessary to examine this novel pattern in individuals from different RHI-related sports and different types of RHI exposure, as well as placing a greater emphasis on the inclusion of women. While we observed associations with exposure group membership, further work is needed to determine whether RHI-WMH predicts cognitive decline, functional impairment, or biomarker progression over time, and whether it provides incremental prognostic value beyond traditional measures of WMH burden. Future work, including clinicopathological research correlating in vivo MRI, *ex vivo* MRI and neuropathology is needed to fully understand the relationship between these lesions and neuropathological correlates.

5 | CONCLUSIONS

In two separate aging cohorts, we found that exposure to RHI was associated with small, punctate, discrete WMH at the depths of the sulci near the gray/white boundary (i.e., RHI-WMH). RHI may be associated with a distinct pattern on T2-FLAIR MRI, offering a potentially valuable tool for clinical assessment and detection of RHI-related neurological conditions.

AFFILIATIONS

[1]Department of Neurology, Boston University Chobanian & Avedisian School of Medicine, Boston, Massachusetts, USA

[2]Boston University Alzheimer's Disease Research Center and BU CTE Center, Boston, Massachusetts, USA

[3]Taub Institute for Research on Alzheimer's Disease and the Aging Brain, Department of Neurology, Vagelos College of Physicians and Surgeons, Columbia University, New York, New York, USA

[4]Department of Radiology, Boston University Chobanian & Avedisian School of Medicine, Boston, Massachusetts, USA

[5]Department of Radiology, Boston Medical Center, Boston, Massachusetts, USA

[6]Department of Biostatistics, Boston University School of Public Health, Boston, Massachusetts, USA

[7]Department of Neurology, Mayo Clinic Arizona, Scottsdale, Arizona, USA

[8]Department of Neurology, NYU Grossman School of Medicine, New York, New York, USA

[9]Department of Population Health and Ophthalmology, NYU Grossman School of Medicine, New York, New York, USA

[10]Cleveland Clinic Lou Ruvo Center for Brain Health, Las Vegas, Nevada, USA

[11]Psychiatry Neuroimaging Laboratory, Department of Psychiatry, Mass General Hospital, Boston, Massachusetts, USA

[12]Department of Psychiatry and Neurochemistry, Institute of Neuroscience and Physiology, The Sahlgrenska Academy at the University of Gothenburg, Gothenburg, Sweden

[13]Banner Research Blood-Based Biomarker Program, Banner Health, Phoenix, Arizona, USA

[14]Department of Neurochemistry, Banner Health, Phoenix, Arizona, USA

[15]Department of Neurodegenerative Disease, University College London Institute of Neurology, London, UK

[16]UK Dementia Research Institute, University College London Institute of Neurology, London, UK

[17]Hong Kong Center for Neurodegenerative Diseases, Hong Kong, China

[18]Wisconsin Alzheimer's Disease Research Center, University of Wisconsin-Madison, Madison, Wisconsin, USA

[19]Clinical Neurochemistry Laboratory, Sahlgrenska University Hospital, Gothenburg, Sweden

[20]Veterans Affairs Northwest Mental Illness Research, Education, and Clinical Center, Seattle, Washington, USA

[21]Department of Psychiatry and Behavioral Sciences, University of Washington School of Medicine, Seattle, Washington, USA

[22]Concussion Legacy Foundation, Boston, Massachusetts, USA

[23]Department of Neurology, Boston Medical Center, Boston, Massachusetts, USA

[24]Department of Neurology, Alzheimer's Disease Research Center, Memory & Aging Center, University of California San Francisco, San Francisco, California, USA

[25]Department of Radiology & Biomedical Imaging, University of California San Francisco, San Francisco, California, USA

[26]Department of Clinical and Health Psychology, University of Florida, Gainesville, Florida, USA

[27]Florida Alzheimer's Disease Research Center, University of Florida, Gainesville, Florida, USA

[28]Department of Pathology and Laboratory Medicine, Boston University Chobanian & Avedisian School of Medicine, Boston, Massachusetts, USA

[29]VA Boston Healthcare System, U.S. Department of Veteran Affairs, Jamaica Plain, Massachusetts, USA

[30]Department of Psychiatry, Boston University Chobanian & Avedisian School of Medicine, Boston, Massachusetts, USA

[31]Department of Pharmacology, Physiology & Biophysics, Boston University Chobanian & Avedisian School of Medicine, Boston, Massachusetts, USA

[32]Department of Ophthalmology, Boston University Chobanian & Avedisian School of Medicine, Boston, Massachusetts, USA

[33]Department of Biomedical, Electrical, and Computer Engineering, Boston University College of Engineering, Boston, Massachusetts, USA

[34]Center for Health Data Science, Boston University School of Public Health, Boston, Massachusetts, USA

[35]Banner Alzheimer's Institute and Arizona Alzheimer's Consortium, Phoenix, Arizona, USA

[36]Department of Software Engineering and Information Technology, École de technologie supérieure, Montreal, QC, Canada

[37]Chambers-Grundy Center for Transformative Neuroscience, Department of Brain Health, Kirk Kerkorian School of Medicine, University of Nevada Las Vegas, Las Vegas, Nevada, USA

[38]Translational Genomics Research Institute, Phoenix, Arizona, USA

[39]Department of Psychiatry, University of Arizona, Phoenix, Arizona, USA

[40]Department of Radiology, Mass General Hospital, Harvard Medical School, Boston, Massachusetts, USA

[41]Department of Anatomy & Neurobiology, Boston University Chobanian & Avedisian School of Medicine, Boston, Massachusetts, USA

[42]Department of Neurosurgery, Boston University Chobanian & Avedisian School of Medicine, Boston, Massachusetts, USA

[43]U.S. Department of Veteran Affairs, VA Bedford Healthcare System, Bedford, Massachusetts, USA

[44]Framingham Heart Study, Boston University Chobanian & Avedisian School of Medicine, Boston, Massachusetts, USA

ACKNOWLEDGMENTS

The authors gratefully acknowledge the generous contributions of time and effort by all of the study participants. This work is supported by the NIA (P30AG072978; R01AG083735), NINDS/NIA (R01NS122854, R01NS139383), and through the Department of Defense (HT9425-24-1-1046). H.Z. is a Wallenberg Scholar and a Distinguished Professor at the Swedish Research Council supported by grants from the Swedish Research Council (#2023-00356, #2022-01018 and #2019-02397), the European Union's Horizon Europe research and innovation programme under grant agreement No 101053962, and Swedish State Support for Clinical Research (#ALFGBG-71320). K.B. is supported by the Swedish Research Council (#2017-00915 and #2022-00732), Hjärnfonden, Sweden (#ALZ2022-0006, #FO2024-0048-TK-130 and FO2024-0048-HK-24), and the Swedish state under the agreement between the Swedish government and the County Councils, the ALF-agreement (#ALFGBG-965240 and #ALFGBG-1006418). B.A. is supported by the UF McKnight Brain Institute, the Norman Fixel Institute for Neurological Diseases, and NIH (P30AG066506; MPI: Smith, Duara, Loewenstein). J.L.C. is supported by NIGMS grant P20GM109025; NIA R35AG71476; Alzheimer's Disease Drug Discovery Foundation (ADDF); Ted and Maria Quirk Endowment; Joy Chambers-Grundy Endowment. J.K.B. has been supported by NIH (RF1AG057768, RF1AG078299, R01AG084624). G.D.R. receives research support from NIH (P30-AG062422, U01-AG057195, R35-AG072362, U01-AG082350), Alzheimer's Association, American College of Radiology, Rainwater Charitable Foundation, Eli Lilly, GE Healthcare, Life Molecular Imaging and Genentech.

CONFLICT OF INTEREST STATEMENT

M.L.A. has received honorarium from the Michael J Fox Foundation Inc., as well as research support from Life Molecular Imaging Inc. He receives royalties from Oxford University Press Inc. R.A. is a scientific advisor to Signant Health and NovoNordisk. H.Z. has served at scientific advisory boards and/or as a consultant for AbbVie, Acumen, Alector, Alzinova, ALZpath, Amylyx, Annexon, Apellis, Artery Therapeutics, AZTherapies, Cognito Therapeutics, CogRx, Denali, Eisai, Enigma, LabCorp, Merck Sharp & Dohme, Merry Life, Nervgen, Novo Nordisk, Optoceutics, Passage Bio, Pinteon Therapeutics, Prothena, Quanterix, Red Abbey Labs, reMYND, Roche, Samumed, ScandiBio Therapeutics AB, Siemens Healthineers, Triplet Therapeutics, and Wave, has given lectures sponsored by Alzecure, BioArctic, Biogen, Cellectricon, Fujirebio, LabCorp, Lilly, Novo Nordisk, Oy Medix Biochemica AB, Roche, and WebMD, is a co-founder of Brain Biomarker Solutions in Gothenburg AB (BBS), which is a part of the GU Ventures Incubator Program, and is a shareholder of MicThera (outside submitted work). K.B. has served as a consultant and on advisory boards for AbbVie, AC Immune, ALZPath, AriBio, Beckman-Coulter, BioArctic, Biogen, Eisai, Lilly, Moleac Pte. Ltd., Neurimmune, Novartis, Ono Pharma, Prothena, Quanterix, Roche Diagnostics, Sunbird Bio, Sanofi and Siemens Healthineers; has served at data monitoring committees for Julius Clinical and Novartis; has given lectures, produced educational materials and participated in educational programs for AC Immune, Biogen, Celdara Medical, Eisai and Roche Diagnostics; and is a co-founder of Brain Biomarker Solutions in Gothenburg AB (BBS), which is a part of the GU Ventures Incubator Program, outside the work presented in this paper. A.M.B. is a scientific advisor/consultant for CogniScreen, Tau Biosciences, Inc., Cognito Terapeutics, Inc., IQVIA, CogState, and Cognition Therapeutics, Inc. He is the inventor of patent for white matter hyperintensity quantification (US Patent US9867566B2). C.J.N. is a volunteer member of the Mackey-White Health & Safety Committee of the National Football League Players Association for which he receives travel support; he has received travel support from the NFL, NFL Players Association, World Rugby, WWE, Total Nonstop Action and AEW for lectures or conferences. C.J.N. is an advisor and options-holder with Oxeia Biopharmaceuticals, LLC, and StataDx; and C.J.N. has served as an expert witness in cases related to concussion and CTE and is compensated for speaking appearances and serving on the Players Advocacy Committee for the NFL Concussion Settlement. C.J.N. is employed by the Concussion Legacy Foundation, a 501(c)(3) non-profit that receives charitable donations. A.E.B. is a consultant or has consulted for Eli Lilly and AbbVie; he receives or has received grant funding from VoxNeuro, and Bristol Myers Squibb; and he receives book royalties from Elsevier and Oxford University Press. J.L.C. has provided consultation to Acadia, Acumen, ALZpath, AnnovisBio, Artery, Axsome, Biogen, Biohaven, Bristol-Myers Squibb, Eisai, Fosun, GAP Foundation, Hummingbird Diagnostics. I.G.C., Janssen, Julius Clinical, Kinoxis, Lighthouse, Lilly, Lundbeck, LSP/eqt, Merck, MoCA Cognition, Novo Nordisk, NSC Therapeutics, Optoceutics, Otsuka, Praxis, ReMYND, Roche, Scottish Brain Sciences, Signant Health, Simcere, Sinaptica, T-Neuro, TrueBinding, and Vaxxinity pharmaceutical, assessment, and investment companies. C.W.F. is a consultant for Boston Imaging Core Lab, LLC. R.A.S. has provided consultation to Biogen, Eisai, Eli Lilly, and Lundbeck. He receives royalties from Psychological Assessment Resources, Inc., and is on the Board of King-Devick Technologies, Inc. G.D.R. has served as a paid consultant for Alector, Bristol Myers Squibb, C2N, Eli Lilly, Johnson & Johnson, Merck, Novo Nordisk and Roche. He has served as a paid speaker for Medscape and Peerview. He is an Associate Editor for JAMA. C.B. receives research support from the UFC, Top Rank Promotions, and Haymon Boxing. The other authors declare no conflicts of interest. Author disclosures are available in the Supporting Information.

CONSENT STATEMENT

All sites received approval from their institutional review board. Participants and/or their legally authorized representative provided written informed consent.

ORCID

Jenna R. Groh https://orcid.org/0000-0002-1831-9314

REFERENCES

1. Daneshvar DH, Nair ES, Baucom ZH, et al. Leveraging football accelerometer data to quantify associations between repetitive head impacts and chronic traumatic encephalopathy in males. *Nat Commun*. 2023;14(1):3470. doi:10.1038/s41467-023-39183-0

2. Nowinski CJ, Bureau SC, Buckland ME, et al. Applying the Bradford hill criteria for causation to repetitive head impacts and chronic traumatic encephalopathy. *Front Neurol*. 2022;13:938163. doi:10.3389/fneur.2022.938163
3. Bieniek KF, Blessing MM, Heckman MG, et al. Association between contact sports participation and chronic traumatic encephalopathy: a retrospective cohort study. *Brain Pathology*. 2020;30(1):63-74. doi:10.1111/bpa.12757
4. Mez J, Daneshvar DH, Abdolmohammadi B, et al. Duration of American Football Play and Chronic Traumatic Encephalopathy. *Ann Neurol*. 2020;87(1):116-131. doi:10.1002/ana.25611
5. McKee AC, Stern RA, Nowinski CJ, et al. The spectrum of disease in chronic traumatic encephalopathy. *Brain*. 2013;136(Pt 1):43-64. doi:10.1093/brain/aws307
6. McKee AC, Stein TD, Kiernan PT, Alvarez VE. The neuropathology of chronic traumatic encephalopathy. *Brain Pathol*. 2015;25(3):350-364. doi:10.1111/bpa.12248
7. Alosco ML, Cherry JD, Huber BR, et al. Characterizing tau deposition in chronic traumatic encephalopathy (CTE): utility of the McKee CTE staging scheme. *Acta Neuropathol*. 2020;140(4):495-512. doi:10.1007/s00401-020-02197-9
8. McKee AC, Alosco ML, Huber BR. Repetitive Head impacts and chronic traumatic encephalopathy. *Neurosurg Clin N Am*. 2016;27(4):529-535. doi:10.1016/j.nec.2016.05.009
9. Pulukuri SV, Fagle TR, Trujillo-Rodriguez D, et al. Characterizing Neurobehavioral Dysregulation Among Former American Football Players: findings from the DIAGNOSE CTE Research Project. *JNP*. doi:10.1176/appi.neuropsych.20230133. Published online July 22, 2024:appi.neuropsych.20230133.
10. Mez J, Alosco ML, Daneshvar DH, et al. Validity of the 2014 traumatic encephalopathy syndrome criteria for CTE pathology. *Alzheimers Dement*. 2021;17(10):1709-1724. doi:10.1002/alz.12338
11. Mez J, Daneshvar DH, Kiernan PT, et al. Clinicopathological evaluation of chronic traumatic encephalopathy in players of American Football. *JAMA*. 2017;318(4):4. doi:10.1001/jama.2017.8334
12. Alosco ML, Stein TD, Tripodis Y, et al. Association of white matter rarefaction, arteriolosclerosis, and tau with dementia in chronic traumatic encephalopathy. *JAMA Neurol*. 2019;76(11):1298-1308. doi:10.1001/jamaneurol.2019.2244
13. Holleran L, Kim JH, Gangolli M, et al. Axonal disruption in white matter underlying cortical sulcus tau pathology in chronic traumatic encephalopathy. *Acta Neuropathol*. 2017;133(3):367-380. doi:10.1007/s00401-017-1686-x
14. Omalu BI, DeKosky ST, Minster RL, Kamboh MI, Hamilton RL, Wecht CH. Chronic traumatic encephalopathy in a National Football League player. *Neurosurgery*. 2005;57(1):128-134. doi:10.1227/01.neu.0000163407.92769.ed. discussion 128-134.
15. Doherty CP, O'Keefe E, Wallace E, et al. Blood–Brain barrier dysfunction as a hallmark pathology in chronic traumatic encephalopathy. *J Neuropathol Exp Neurol*. 2016;75(7):656-662. doi:10.1093/jnen/nlw036
16. Alosco ML, Ly M, Mosaheb S, et al. Decreased myelin proteins in brain donors exposed to football-related repetitive head impacts. *Brain Commun*. 2023;5(2):fcad019. doi:10.1093/braincomms/fcad019
17. Duering M, Biessels GJ, Brodtmann A, et al. Neuroimaging standards for research into small vessel disease—advances since 2013. *Lancet Neurol*. 2023;22(7):602-618. doi:10.1016/S1474-4422(23)00131-X
18. Eloyan A, Thangarajah M, An N, et al. White matter hyperintensities are higher among early-onset Alzheimer's disease participants than their cognitively normal and early-onset nonAD peers: longitudinal Early-onset Alzheimer's Disease Study (LEADS). *Alzheimers Dement*. 2023;25. doi:10.1002/alz.13402. Published online July.
19. Schoemaker D, Zanon Zotin MC, Chen K, et al. White matter hyperintensities are a prominent feature of autosomal dominant Alzheimer's disease that emerge prior to dementia. *Alzheimers Res Ther*. 2022;14(1):89. doi:10.1186/s13195-022-01030-7
20. Dadar M, Manera AL, Ducharme S, Collins DL. White matter hyperintensities are associated with grey matter atrophy and cognitive decline in Alzheimer's disease and frontotemporal dementia. *Neurobiol Aging*. 2022;111:54-63. doi:10.1016/j.neurobiolaging.2021.11.007
21. Lee S, Viqar F, Zimmerman ME, et al. White matter hyperintensities are a core feature of Alzheimer's disease: evidence from the dominantly inherited Alzheimer network. *Annals of Neurology*. 2016;79(6):929-939. doi:10.1002/ana.24647
22. Alber J, Alladi S, Bae HJ, et al. White matter hyperintensities in vascular contributions to cognitive impairment and dementia (VCID): knowledge gaps and opportunities. *Alzheimers Dement (N Y)*. 2019;5:107-117. doi:10.1016/j.trci.2019.02.001
23. Alosco ML, Tripodis Y, Baucom ZH, et al. White matter hyperintensities in former American football players. *Alzheimers Dement*. 2023;19(4):1260-1273. doi:10.1002/alz.12779
24. Alosco ML, Koerte IK, Tripodis Y, et al. White matter signal abnormalities in former National Football League players. *Alzheimers Dement (Amst)*. 2017;10:56-65. doi:10.1016/j.dadm.2017.10.003
25. Ly MT, Tuz-Zahra F, Tripodis Y, et al. Association of vascular risk factors and CSF and imaging biomarkers with white matter hyperintensities in former American football players. *Neurology*. 2024;102(2):e208030. doi:10.1212/WNL.0000000000208030
26. Miner AE, Groh JR, Farris C, et al. Does white matter and vascular injury from repetitive head impacts lead to a novel pattern on T2 FLAIR MRI? A hypothesis proposal and call for research. *Alzheimers Dement*. 2025;21(3):e70085. doi:10.1002/alz.70085
27. Alosco ML, Adler CH, Balcer LJ, et al. Developing methods to detect and diagnose chronic traumatic encephalopathy during life: rationale, design, and methodology for the DIAGNOSE CTE Research Project. *Alzheimers Res Ther*. 2021;13(1):136. doi:10.1186/s13195-021-00872-x
28. Alosco ML, Mariani ML, Adler CH, et al. Developing methods to detect and diagnose chronic traumatic encephalopathy during life: rationale, design, and methodology for the DIAGNOSE CTE Research Project. *Alzheimers Res Ther*. 2021;13:136. doi:10.1186/s13195-021-00872-x
29. Su Y, Protas H, Luo J, et al. Flortaucipir tau PET findings from former professional and college American football players in the DIAGNOSE CTE research project. *Alzheimers Dement*. 2024;20(3):1827-1838. doi:10.1002/alz.13602
30. Fischl B, Salat DH, Busa E, et al. Whole brain segmentation: automated labeling of neuroanatomical structures in the human brain. *Neuron*. 2002;33(3):341-355. doi:10.1016/s0896-6273(02)00569-x
31. Fleisher AS, Chen K, Liu X, et al. Using positron emission tomography and florbetapir F18 to image cortical amyloid in patients with mild cognitive impairment or dementia due to Alzheimer disease. *Arch Neurol*. 2011;68(11):1404-1411. doi:10.1001/archneurol.2011.150
32. Cm C, Ja S, Bj B, et al. Use of florbetapir-PET for imaging beta-amyloid pathology. *JAMA*. 2011;305(3). doi:10.1001/jama.2010.2008
33. Stern RA, Adler CH, Chen K, et al. Tau Positron-emission tomography in former national football league players. *N Engl J Med*. 2019;380(18):1716-1725. doi:10.1056/NEJMoa1900757
34. Stern RA, Trujillo-Rodriguez D, Tripodis Y, et al. Amyloid PET across the cognitive spectrum in former professional and college American football players: findings from the DIAGNOSE CTE Research Project. *Alzheimers Res Ther*. 2023;15(1):166. doi:10.1186/s13195-023-01315-5
35. Ashton NJ, Pascoal TA, Karikari TK, et al. Plasma p-tau231: a new biomarker for incipient Alzheimer's disease pathology. *Acta Neuropathol*. 2021;141(5):709-724. doi:10.1007/s00401-021-02275-6
36. Miner AE, Groh JR, Tripodis Y, et al. Examination of plasma biomarkers of amyloid, tau, neurodegeneration, and neuroinflammation in former elite American football players. *Alzheimers Dement*. 2024;20(11):7529-7546. doi:10.1002/alz.14231

37. van Gennip ACE, Satizabal CL, Tracy RP, et al. Associations of plasma NfL, GFAP, and t-tau with cerebral small vessel disease and incident dementia: longitudinal data of the AGES-Reykjavik Study. *GeroScience*. 2023;46(1):505-516. doi:10.1007/s11357-023-00888-1
38. Asken BM, Tanner JA, Gaynor LS, et al. Alzheimer's pathology is associated with altered cognition, brain volume, and plasma biomarker patterns in traumatic encephalopathy syndrome. *Alzheimers Res Ther*. 2023;15(1):126. doi:10.1186/s13195-023-01275-w
39. van Amerongen S, Pulukuri SV, Tuz-Zahra F, et al. Inflammatory biomarkers for neurobehavioral dysregulation in former American football players: findings from the DIAGNOSE CTE Research Project. *J Neuroinflammation*. 2024;21(1):46. doi:10.1186/s12974-024-03034-6
40. Asken BM, Tanner JA, VandeVrede L, et al. Plasma P-tau181 and P-tau217 in patients with traumatic encephalopathy syndrome with and without evidence of Alzheimer Disease Pathology. *Neurology*. 2022;99(6):e594-e604. doi:10.1212/WNL.0000000000200678
41. Teunissen CE, Verberk IMW, Thijssen EH, et al. Blood-based biomarkers for Alzheimer's disease: towards clinical implementation. *Lancet Neurol*. 2022;21(1):66-77. doi:10.1016/S1474-4422(21)00361-6
42. Katz DI, Bernick C, Dodick DW, et al. National Institute of Neurological Disorders and Stroke consensus diagnostic criteria for traumatic encephalopathy syndrome. *Neurology*. 2021;96(18):848-863. doi:10.1212/WNL.0000000000011850
43. Alosco ML, Morrison M, Au R, et al. Boston University Alzheimer's Disease Research Center Clinical Core: infrastructure to facilitate research on post-traumatic Alzheimer's disease and related dementias. *Alzheimers Dement*. 2025;21(9):e70654. doi:10.1002/alz.70654
44. Mez J, Solomon TM, Daneshvar DH, et al. Assessing clinicopathological correlation in chronic traumatic encephalopathy: rationale and methods for the UNITE study. *Alzheimers Res Ther*. 2015;7(1):62. doi:10.1186/s13195-015-0148-8
45. Alosco ML, Mian AZ, Buch K, et al. Structural MRI profiles and tau correlates of atrophy in autopsy-confirmed CTE. *Alzheimers Res Ther*. 2021;13:193. doi:10.1186/s13195-021-00928-y
46. Bruce HJ, Tripodis Y, McClean M, et al. American football play and parkinson disease among men. *JAMA Netw Open*. 2023;6(8):e2328644. doi:10.1001/jamanetworkopen.2023.28644
47. Alosco ML, Jarnagin J, Tripodis Y, et al. Utility of providing a concussion definition in the assessment of concussion history in former NFL players. *Brain Injury*. 2017;31(8):1116-1123. doi:10.1080/02699052.2017.1294709
48. Montenigro PH, Alosco ML, Martin BM, et al. Cumulative head impact exposure predicts later-life depression, apathy, executive dysfunction, and cognitive impairment in former high school and college football players. *J Neurotrauma*. 2017;34(2):328-340. doi:10.1089/neu.2016.4413
49. Bieniek KF, Cairns NJ, Crary JF, et al. The second NINDS/NIBIB consensus meeting to define neuropathological criteria for the diagnosis of chronic traumatic encephalopathy. *J Neuropathol Exp Neurol*. 2021;80(3):210-219. doi:10.1093/jnen/nlab001
50. Schmidt P, Pongratz V, Küster P, et al. Automated segmentation of changes in FLAIR-hyperintense white matter lesions in multiple sclerosis on serial magnetic resonance imaging. *Neuroimage Clin*. 2019;23:101849. doi:10.1016/j.nicl.2019.101849
51. Griffanti L, Zamboni G, Khan A, et al. BIANCA (Brain Intensity AbNormality Classification Algorithm): a new tool for automated segmentation of white matter hyperintensities. *NeuroImage*. 2016;141:191-205. doi:10.1016/j.neuroimage.2016.07.018
52. Fazekas F, Chawluk JB, Alavi A, Hurtig HI, Zimmerman RA. MR signal abnormalities at 1.5 T in Alzheimer's dementia and normal aging. *AJR Am J Roentgenol*. 1987;149(2):351-356. doi:10.2214/ajr.149.2.351
53. Scheltens P, Barkhof F, Leys D, et al. A semiquantative rating scale for the assessment of signal hyperintensities on magnetic resonance imaging. *J Neurol Sci*. 1993;114(1):7-12. doi:10.1016/0022-510x(93)90041-v
54. Pan Y, Hamdi M, Li K. Euclidean distance transform for binary images on reconfigurable mesh-connected computers. *IEEE Trans Syst Man Cybern B Cybern*. 2000;30(1):240-244. doi:10.1109/3477.826967
55. Lee J, Jiang JY, Wu W, Lesage F, Boas DA. Statistical intensity variation analysis for rapid volumetric imaging of capillary network flux. *Biomed Opt Express*. 2014;5(4):1160-1172. doi:10.1364/BOE.5.001160
56. Yin X, Ng BWH, He J, Zhang Y, Abbott D. Accurate image analysis of the retina using hessian matrix and binarisation of thresholded entropy with application of texture mapping. *PLoS One*. 2014;9(4):e95943. doi:10.1371/journal.pone.0095943
57. Zhang M, Wu T, Beeman SC, et al. Efficient small blob detection based on local convexity, intensity and shape information. *IEEE Trans Med Imaging*. 2016;35(4):1127-1137. doi:10.1109/TMI.2015.2509463
58. Razlighi QR, Stern Y. Blob-like feature extraction and matching for brain MR images. *Annu Int Conf IEEE Eng Med Biol Soc*. 2011;2011:7799-7802. doi:10.1109/IEMBS.2011.6091922
59. Schwartzman A, Jaffe A, Gavrilov Y, Meyer CA. Multiple testing of local maxima for detection of peaks in ChIP-seq data. *Ann Appl Stat*. 2013;7(1):471-494. doi:10.1214/12-aoas594
60. Dufouil C, Beiser A, McLure LA, et al. A revised framingham stroke risk profile to reflect temporal trends. *Circulation*. 2017;135(12):1145-1159. doi:10.1161/CIRCULATIONAHA.115.021275
61. Alosco ML, Mez J, Tripodis Y, et al. Age of first exposure to tackle football and chronic traumatic encephalopathy. *Ann Neurol*. 2018;83(5):5. doi:10.1002/ana.25245
62. Cherry JD, Tripodis Y, Alvarez VE, et al. Microglial neuroinflammation contributes to tau accumulation in chronic traumatic encephalopathy. *Acta Neuropathologica Communications*. 2016;4(1):112. doi:10.1186/s40478-016-0382-8
63. Butler MLMD, Pervaiz N, Ypsilantis P, et al. Repetitive head impacts induce neuronal loss and neuroinflammation in young athletes. *bioRxiv*. Published online March 28, 2024. doi:10.1101/2024.03.26.586815
64. Albayram O, Kondo A, Mannix R, et al. Cis P-tau is induced in clinical and preclinical brain injury and contributes to post-injury sequelae. *Nat Commun*. 2017;8(1):1000. doi:10.1038/s41467-017-01068-4

SUPPORTING INFORMATION

Additional supporting information can be found online in the Supporting Information section at the end of this article.

How to cite this article: Groh JR, Miner AE, Alshikho MJ, et al. Imaging the later-life white matter pathologies of repetitive head impacts: A novel pattern revealed through T2 FLAIR MRI. *Alzheimer's Dement*. 2026;22:e71351. https://doi.org/10.1002/alz.71351